

Full Length Research Paper

Combined influence of Soret and Dufour effects on convective heat and mass transfer flow through a porous medium in cylindrical annulus with heat sources

P. Sudarsan Reddy^{1*} and D. R. V. Prasada Rao²

¹Department of Mathematics, RGM (Rajeev Gandhi Memorial) Engineering College, Nandyal, India.

²Department of Mathematics, Sri Krishnadevaraya (SK) University, Anantapur, India.

Accepted 5 August, 2010

The heat and mass transfer characteristics of non-Darcy mixed convective flow of a viscous electrically conducting fluid through a porous medium in a circular cylindrical annulus in the presence of temperature gradient heat sources with Soret and Dufour effects have been analyzed. The partial differential equations governing the problem under consideration are transformed into a system of ordinary differential equations and are solved numerically by using the Galerkin finite element method. The velocity, temperature and concentration profiles are presented graphically for various values of the parameters.

Key words: Heat transfer, mass transfer, Soret effects, Dufour effect, and temperature gradient heat sources.

INTRODUCTION

Convection flows driven by temperature and concentration differences have been studied extensively in the past and various extensions of the problems have been reported in the literature. With both temperature and concentration interacting simultaneously, the convection has become quite complex. Bejan and Khair [1985] have investigated the vertical free convection flow embedded in a porous medium resulting from the combined heat and mass transfer. Jang and Chang [1987] have used an implicit finite difference method to study the buoyancy induced inclined boundary layer in a porous medium resulting from the combined heat and mass buoyancy effects.

Heat transfers in thermal insulation within vertical cylindrical annuli provide us insight into the mechanism of energy transport and enable engineers to use insulation more efficiently. In particular design engineers require

relationship between heat transfer, geometry and boundary conditions which can utilize cost-benefit analysis to determine the amount of insulation that will yield the maximum investment.

An understanding of convective heat transfer in porous annuli is essential for its applications in packed-bed catalytic reactors, geo-physics, thermal insulation, design of regenerative heat exchangers, geological disposal of high-level nuclear waste, petroleum resources and many other uses. Free convection in a vertical porous annulus has been extensively studied by Prasad [1984], Prasad and Kulacki [1985] and Prasad et al. [1985] both theoretically and experimentally. Convection through annular regions under steady conditions has also been discussed with the two cylindrical surfaces kept at different temperatures [Bejan and Lazzari, 1985]. This work has been extended in temperature dependent convection flow [Muthukumara et al., 2007] as well as convection flow through horizontal porous channel whose inner surface is maintained at constant temperature, while the other surface is maintained at circumferentially varying

*Corresponding author. E-mail: suda1983@gmail.com.

sinusoidal temperature [Vasseur et al., 1984].

The application of electromagnetic fields in controlling the heat transfer as in aerodynamic heating leads to the study of Magneto hydrodynamic heat transfer. This MHD heat transfer has gained significance owing to recent advancement of space technology. The MHD heat transfer can be divided into two sections. One contains problems in which the heating is an incidental by product of the electromagnetic fields as in MHD generators and pumps etc. and the second consists of problems in which the primary use of electromagnetic fields is to control the heat transfer [Chandra, 1961]. With fuel crisis deepening all over the world, there is a great concern to utilize the enormous power beneath the earth's crust in the geothermal region [Nanda and Mohan, 1978]. Liquid in the geothermal region is an electrically conducting liquid because of high temperature and that they undergo the influence of magnetic field.

In many industrial applications of transient free convection flow problems, there occurs a heat source or a sink which is either a constant or temperature gradient or temperature dependent heat source. This heat source occurs in the form of a coil or a battery. Gokhale and Behnaz-Farman [2007] analyzed transient free convection flow of an incompressible fluid past an isothermal plate with temperature gradient dependent heat sources. Implicit finite difference scheme which is unconditionally stable has been used to solve the governing partial differential equations of the flow. Transient temperature and velocity profiles are plotted to show the effect of heat source. Muthukumara et al. [2007] have analyzed the radiation effect on moving vertical plate with variable temperature and mass diffusion. Sreevani [2003] has analyzed the Soret effect on convective heat and mass transfer flow of a viscous fluid in a cylindrical annulus with heat generating sources. Sivaiah [2004] has discussed the convective heat and mass transfer flow in a circular duct with Soret effect.

Literature suggests that the effect of viscous dissipation on heat transfer has been studied for different geometries. Brinkman [1948] has studied the viscous dissipation effect on natural convection in horizontal cylinder embedded in porous medium. Their study showed that the viscous dissipation effect might not be neglected. Saffman [1971] has studied the viscous dissipation effect on natural convection in a porous cavity and found that the heat transfer rate at hot surface decreases with increase of viscous dissipation parameter. Thermal radiation plays a significant role in the overall surface heat transfer where convective heat transfer is small. Verschoor [1992] have studied the effect of viscous dissipation and radiation on unsteady magneto hydro dynamic free convection flow past vertical plate in porous medium. They found that the temperature profile increases when viscous dissipation increases. A good amount of work has been done to understand natural

convection in porous cavity. In spite of endeavor efforts to study heat transfer in porous cavity, the combined effect of viscous dissipation and radiation on porous medium filled inside a square cavity has not received attention. The Soret and Dufour effects have garnered considerable interest in both Newtonian and non-Newtonian convective heat and mass transfer. Such effects are significant when density differences exist in the flow regime. Soret and Dufour effects are important for intermediate molecular weight gases in coupled heat and mass transfer in binary systems, often encountered in chemical process engineering and also in high-speed aerodynamics. Soret and Dufour effects are also critical in various porous flow regimes occurring in chemical and geophysical systems. There are few studies about the Soret and Dufour effects in a Darcy or non-Darcy porous medium. Anghel et al. [2000] have examined the composite Soret and Dufour effects on free convective heat and mass transfer in a Darcian porous medium with Soret and Dufour effects. Recently, Barletta et al. [2008] have studied on mixed convection with heating effects in a vertical porous annulus with a radially varying magnetic field. Emmunuel et al. [2008] have discussed Thermal-diffusion and diffusion thermo effects on combined heat and mass transfer of a steady MHD convective and slip flow due to a rotating disk with viscous dissipation and ohmic heating. Very recently, Sallam (2009) has analysed thermal-diffusion and diffusion-thermo effects on mixed convection heat and mass transfer in a porous medium.

The weighted residual method is of the generalization of the Ritz-variational method wherein we seek an approximate solution in the form of linear combination of suitable approximation functions. The parameters in the linear combination are determined by setting integral of a weighted residual of the approximation over the domain zero. A comprehensive description of a weighted residual method has been given. In many situations the Galerkin method which is one of the important weighted residual methods is equivalent to the Ritz method for solving variational problems. The finite Element method is piece-wise application of weighted residual method in which the Ritz-Galerkin type methods are employed over each element of the domain. The finite element method was initially developed as an adhoc engineering procedure for constructing matrix solutions to stress and displacement calculations in structural analysis. Very few fluid dynamic problems can be expressed in a variational form. Consequently, most of the finite element applications in fluid dynamics have been used in Galerkin finite element formulation. The Galerkin finite element method has two important features. Firstly the approximate solution is written directly as a linear combination of approximating functions in terms of the nodal unknowns. Secondly the approximating functions or the shape functions are chosen exclusively from low order piecewise polynomials restricted to contiguous elements.

In this paper we discuss the mixed convective viscous dissipative flow through a porous medium in a circular cylindrical annulus with Thermal-Diffusion and Diffusion-Thermo effects in the presence of temperature gradient heat source, where the inner wall maintained constant temperature and the outer wall maintained constant heat flux, with the concentration being constant on both walls. The coupled momentum, energy and diffusion equations are solved by using finite element analysis with quadratic interpolation polynomials. The effect of temperature gradient heat sources on the flow and heat transfer characteristics are analyzed. The stress, rate of heat transfer and the rate of mass transfer are discussed numerically for different variations of the governing parameters.

FORMULATION OF THE PROBLEM

We consider free and force convective flow of a viscous, electrically conducting fluid through a porous medium in a circular cylindrical annulus with Thermal-Diffusion and Diffusion-Thermo effects in the presence of temperature gradient heat source, whose inner wall is maintained at a constant temperature and the outer wall is maintained at constant heat flux. Also the concentration is constant on the both walls. A uniform radial magnetic field is applied on the flow. The flow, temperature and concentration in the fluid are assumed to be fully developed. Both the fluid and porous region have constant physical properties and the flow is a mixed convection flow taking place under thermal and molecular buoyancies and uniform axial pressure gradient. The boussenisque approximation is invoked so that the density variation is confined to the thermal and molecular buoyancy forces. The Brinkman-Forchhimer-Extended Darcy model which accounts for the inertia and boundary effects has been used for the momentum equation in the porous region. In the momentum, energy and diffusion are coupled and non-linear. Also the flow in is unidirectional along the axial cylindrical annulus. Making use of the above assumptions the governing equations are:

Equation of linear momentum

$$-\frac{\partial p}{\partial z} + \frac{\mu}{\delta} \left(\frac{\partial^2 u}{\partial r^2} + \frac{1}{r} \frac{\partial u}{\partial r} \right) - \frac{\mu}{k} u - \frac{\rho \delta F}{\sqrt{k}} u^2 + \rho g \beta (T - T_0) + \rho g \beta^* (C - C_0) + \frac{\sigma \mu_e^2 H_0^2}{\gamma} u = 0 \quad (1)$$

Equation of energy

$$\rho_p \mu \frac{\partial T}{\partial z} = \lambda \left(\frac{\partial^2 T}{\partial r^2} + \frac{1}{r} \frac{\partial T}{\partial r} \right) + \frac{Q \partial T}{r \partial r} + \mu \left(\frac{\partial u}{\partial r} \right)^2 + \frac{D_m K_t}{C_s C_p} \left(\frac{\partial^2 C}{\partial r^2} + \frac{1}{r} \frac{\partial C}{\partial r} \right) \quad (2)$$

Equation of diffusion

$$u \frac{\partial C}{\partial z} = D_1 \left(\frac{\partial^2 C}{\partial r^2} + \frac{1}{r} \frac{\partial C}{\partial r} \right) + \frac{D_m K_t}{T_m} \left(\frac{\partial^2 T}{\partial r^2} + \frac{1}{r} \frac{\partial T}{\partial r} \right) \quad (3)$$

Equation of state

$$\rho - \rho_0 = -\beta \rho_0 (T - T_0) - \beta^* \rho_0 (C - C_0) \quad (4)$$

Where u is the axial velocity in the porous region, T and C are the temperature and concentrations of the fluid, k is the permeability of porous medium, F is a function that depends on Reynolds number and the microstructure of the porous medium and D_1 is the Molecular diffusivity, D_m is the coefficient of mass diffusivity, T_m is the mean fluid temperature, K_t is the thermal diffusion, C_s is the concentration susceptibility, C_p is the specific heat, ρ is density, g is gravity, β is the coefficient of thermal expansion, β^* is the coefficient of volume expansion, σ is the electrical conductivity, μ_e is the magnetic permeability.

$$u = 0, \quad T = T_i, \quad C = C_i \quad \text{at } r = a \quad (5)$$

$$u = 0, \quad \frac{\partial T}{\partial r} = Q_1, \quad C = C_0 \quad \text{at } r = a + s \quad (6)$$

The axial temperature gradient $\frac{\partial T}{\partial z}$ and concentration

gradient $\frac{\partial C}{\partial z}$ are assumed to be constant, say A and respectively. Using Equations (5) and (6), Equations (2) and (3) reduce to

$$\rho_0 C_p u A = \lambda \left(T_{rr} + \frac{1}{r} T_r \right) + \frac{D_m K_t}{C_s C_p} \left(C_{rr} + \frac{1}{r} C_r \right) \quad (7)$$

$$\rho_0 C_p u B = \lambda \left(C_{rr} + \frac{1}{r} C_r \right) + \frac{D_m K_t}{C_s C_p} \left(T_{rr} + \frac{1}{r} T_r \right) \quad (8)$$

We now define the following non-dimensional variables

$$z^* = \frac{z}{a}, \quad r^* = \frac{r}{a}, \quad u^* = \frac{a}{v} u, \quad p^* = \frac{pa \delta}{\rho v^2}$$

$$\theta^* = \frac{T - T_i}{T_i - T_0}, \quad C^* = \frac{C - C_i}{C_i - C_0}, \quad s^* = \frac{s}{a} \quad (9)$$

Introducing these non-dimensional variables, the

governing equations in the non-dimensional form are (on removing the stars):

$$\frac{d^2 u}{dr^2} + \frac{1}{r} \frac{du}{dr} = P + \delta \left(D^{-1} + \frac{M^2}{r^2} \right) u + \delta^2 \Lambda u^2 - \delta G \theta \quad (10)$$

$$\frac{d^2 \theta}{dr^2} + \frac{1}{r} \frac{d\theta}{dr} + \frac{\alpha d\theta}{r dr} = P_r N_t u + D N_t \left(\frac{d^2 C}{dr^2} + \frac{1}{r} \frac{dC}{dr} \right) + P_r E_c \left(\frac{du}{dr} \right)^2 \quad (11)$$

$$\frac{d^2 C}{dr^2} + \frac{1}{r} \frac{dC}{dr} = S_c N_c u + S_c S_r \left(\frac{d^2 \theta}{dr^2} + \frac{1}{r} \frac{d\theta}{dr} \right) \quad (12)$$

where $\Lambda = FD^{-1}$ (Forchheimer number)

$$P_r = \frac{\mu C_p}{\lambda} \quad (\text{Prandtl number})$$

$$G = \frac{g\beta(T_1 - T_0)a^3}{\nu^2} \quad (\text{Grashof number})$$

$$D^{-1} = \frac{a^2}{k} \quad (\text{Inverse Darcy parameter})$$

$$N_t = \frac{Aa}{T_1 - T_0} \quad (\text{Temperature gradient})$$

$$N_c = \frac{Ba}{C_1 - C_0} \quad (\text{Non-dimensional concentration gradient})$$

$$Du = \left(\frac{D_m K_r \Delta c a^2}{C_s C_p \Delta T \lambda} \right) \quad (\text{Dufour Number})$$

$$Sc = \frac{\nu}{D_1} \quad (\text{Schmidt number})$$

$$\alpha = \frac{QL^2}{\lambda C_p} \quad (\text{Heat source parameter})$$

$$M^2 = \frac{\sigma \mu_e^2 H_0^2 a^2}{\gamma^2} \quad (\text{Hartman number})$$

$$E_c = \frac{v^2}{a^2 (Aa) c_p} \quad (\text{Eckert number})$$

With the corresponding boundary conditions as:

$$u = 0, \quad \theta = 0, \quad C = 1 \quad \text{at } r = 1 \quad (13)$$

$$u = 0, \quad \frac{\partial \theta}{\partial r} = Q_1, \quad C = 0 \quad \text{at } r = 1 + s \quad (14)$$

NUMERICAL ANALYSIS

The finite element method has been implemented to obtain numerical solutions of Equations (11) to (13) under boundary conditions (14) and (15). This technique is extremely efficient and allows robust solutions of complex coupled, nonlinear multiple degree differential equation systems. The fundamental steps comprising the method are now summarized:

- Phase 1. Discretization of the domain into elements
- Phase 2. Derivation of element equations
- Phase 3. Assembly of Element Equations
- Phase 4. Imposition of boundary conditions
- Phase 5. Solution of assembled equations

The shear stress are evaluated on the cylinder using the formula,

$$\tau = \left(\frac{du}{dr} \right)_{r=1,1+s}$$

The rates of heat transfer (Nusselt number) are evaluated on the cylinder using the formula,

$$Nu = - \left(\frac{d\theta}{dr} \right)_{r=1}$$

The rate of mass transfer (Sherwood Number) is evaluated using the formula,

$$Sh = - \left(\frac{dC}{dr} \right)_{r=1,1+s}$$

DISCUSSION OF THE NUMERICAL RESULTS

In this analysis we investigate thermo-Diffusion and Diffusion-Thermo effects on convective heat and mass transfer flow of a viscous conducting fluid through a porous medium in circular annulus in the presence of temperature gradient dependent heat source with viscous dissipation. The inner cylinder is maintained at constant temperature, the outer wall is maintained at constant heat flux while the concentration is maintained constant on both the cylinders. The axial flow is in vertically down ward direction, $u > 0$ indicates a reversal flow. The velocity, temperature and concentration distributions are shown in Figures 1-27 for different values of the parameters $G, D^{-1}, M, Sc, Sr, Du, N, \alpha$ and E_c .

The variation of u with Grashof number G shows that the axial flow enhances increase in G and the region of reversal flow enhances increase in G (Figure 1).

With respect to the variation of u with D^{-1} we found that

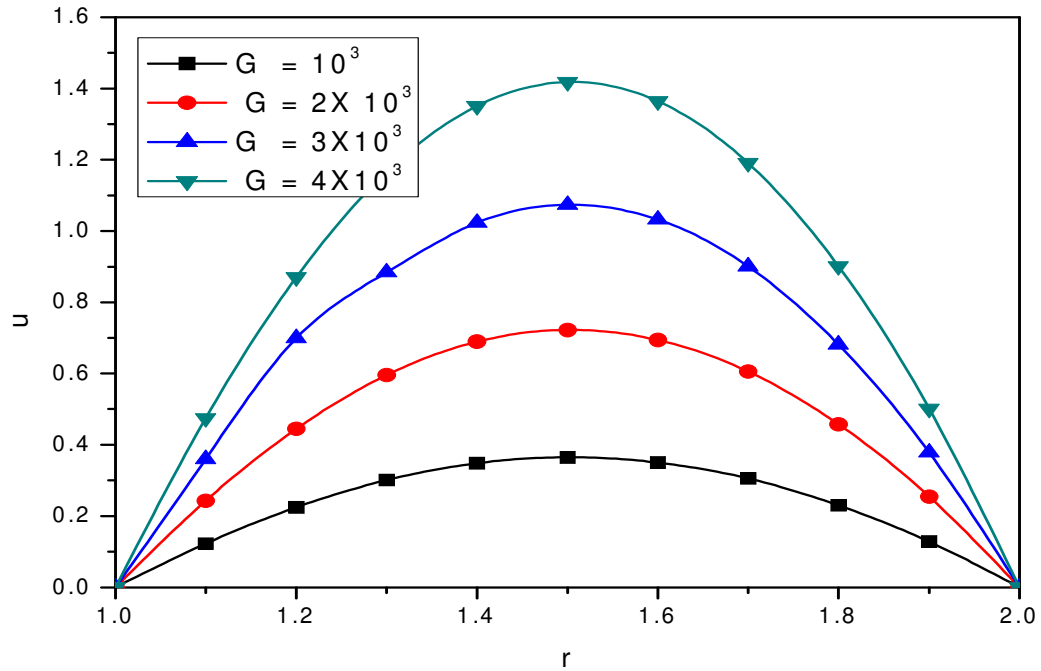


Figure 1. Variation of u with G $P = 0.71$, $Sr = 0.5$, $D^{-1} = 2 \times 10^3$, $M = 2$, $\alpha = 2$, $N = 2$, $Du = 0.5$, $Ec = 0.01$, $Sc = 1.3$.

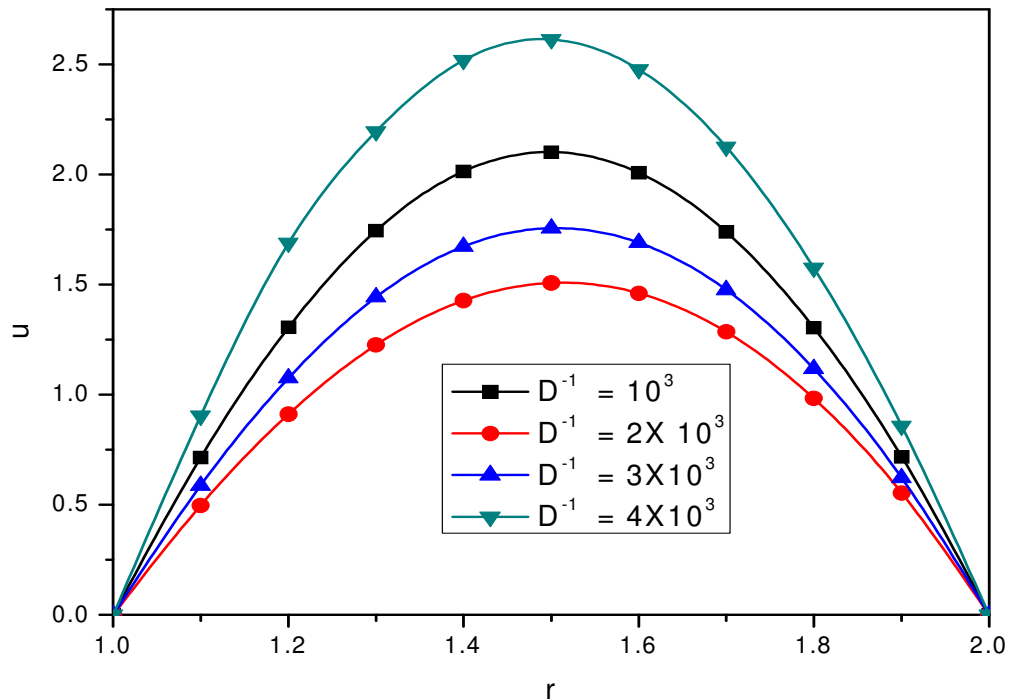


Figure 2. Variation of u with D^{-1} $P = 0.71$, $Sr = 0.5$, $G = 2 \times 10^3$, $\alpha = 2$, $M = 2$, $N = 2$, $Du = 0.5$, $Ec = 0.01$, $Sc = 1.3$.

the lesser the permeability of porous medium, the smaller the magnitude of u ; and for further lowering of the permeability, the larger the magnitude of u in the entire

flow region, the more the region of reversal flow shrinks with $D^{-1} \leq 2 \times 10^3$ and enhances higher $D^{-1} \geq 3 \times 10^3$ (Figure 2). From Figure 3 we found that the higher the

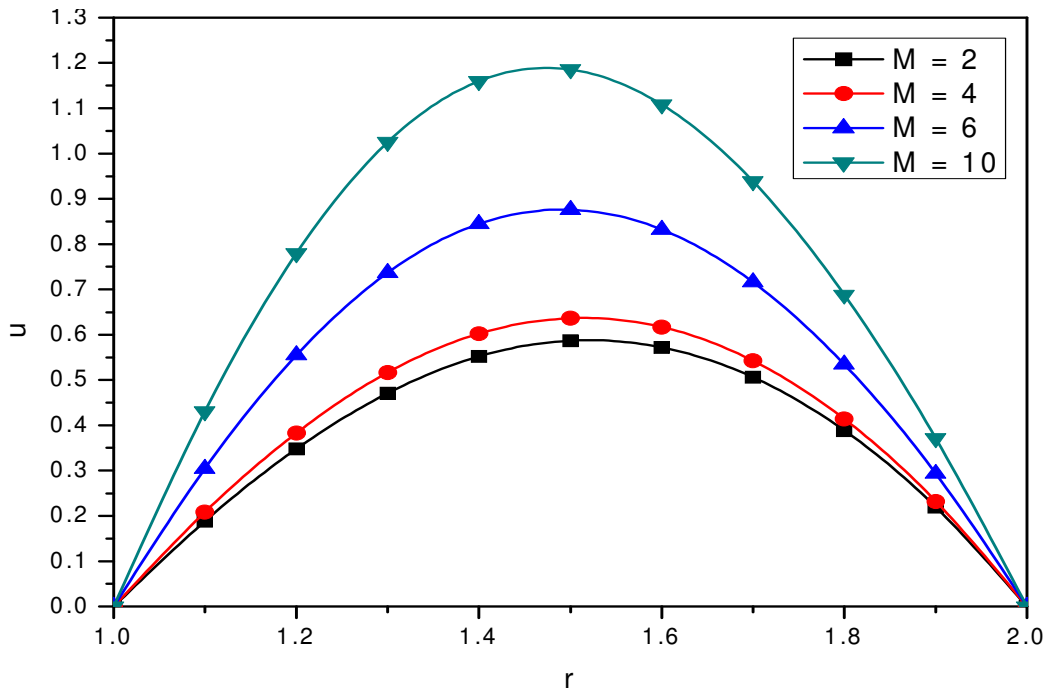


Figure 3. Variation of u with $MP = 0.71$, $Sr = 0.5$, $G = 2 \times 10^3$, $D^{-1} = 2 \times 10^3$, $N = 2$, $\alpha = 2$, $Du = 0.5$, $Ec = 0.01$, $Sc = 1.3$.

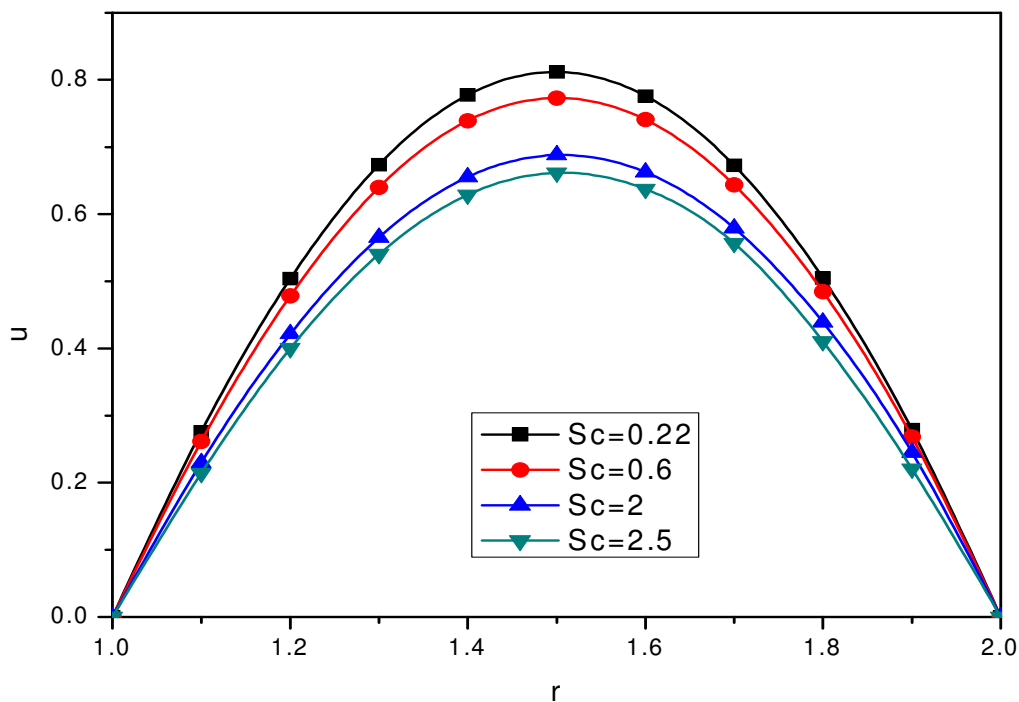


Figure 4. Variation of u with $Sc P = 0.71$, $Sr = 0.5$, $G = 2 \times 10^3$, $M = 2$, $\alpha = 2$, $N = 2$, $Du = 0.5$, $Ec = 0.01$, $D^{-1} = 2 \times 10^3$.

Lorentz force, the larger the velocity in the flow region. Also the region of reversal flow enhances increase in M . Figure 4 represents the variation of u with Sc . We noticed

that the lesser the molecular diffusivity, the smaller the $|u|$; and for further lowering of molecular diffusivity it experiences a depreciation in the entire flow region and

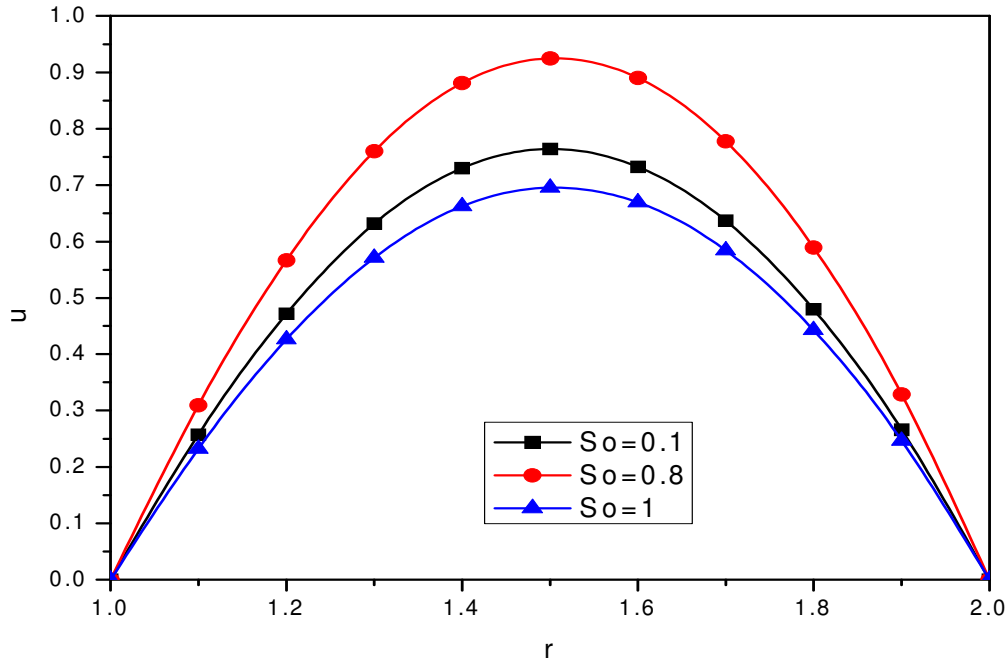


Figure 5. Variation of u with So $P = 0.71$, $D^{-1} = 2 \times 10^3$, $G = 2 \times 10^3$, $M = 2$, $N = 2$, $\alpha = 2$, $Du = 0.5$, $Ec = 0.01$, $Sc = 1.3$.

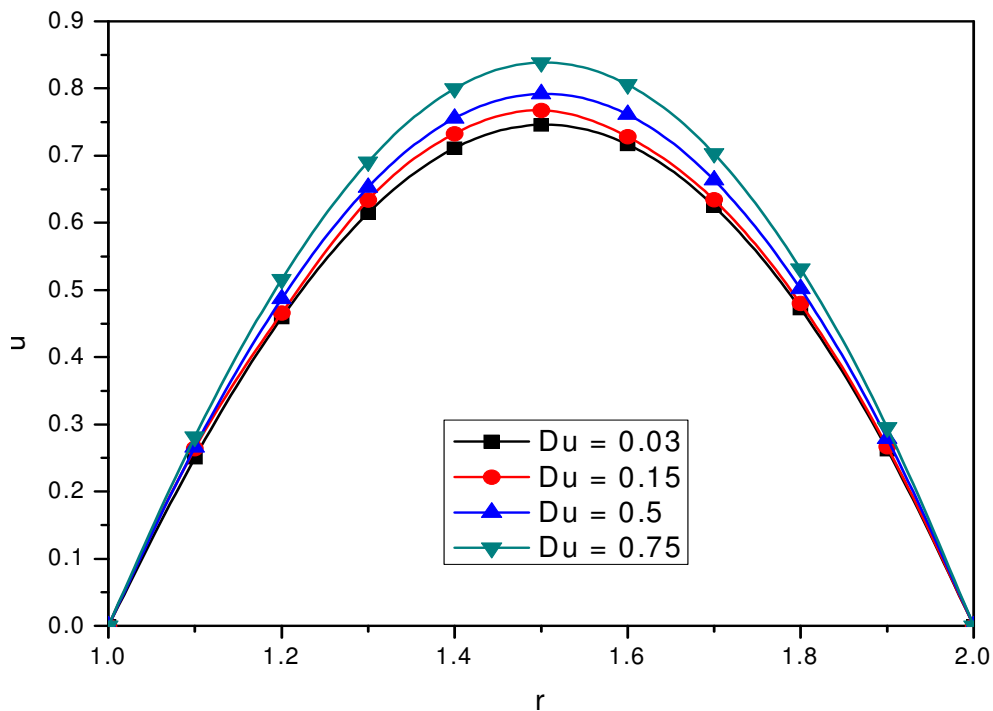


Figure 6. Variation of u with Du $P = 0.71$, $Sr = 0.5$, $G = 2 \times 10^3$, $M = 2$, $N = 2$, $D^{-1} = 2 \times 10^3$, $\alpha = 2$, $Ec = 0.01$, $Sc = 1.3$.

attains maximum at $r = 1.5$.

The variation of u with Soret parameter Sr shows that the velocity experiences an enhancement with increase

in $Sr \leq 0.8$ and for further increase in $Sr \geq 1$ it depreciates in its magnitude (Figure 5). From Figure 6 we observe that the region of reversal velocity enlarges with increase

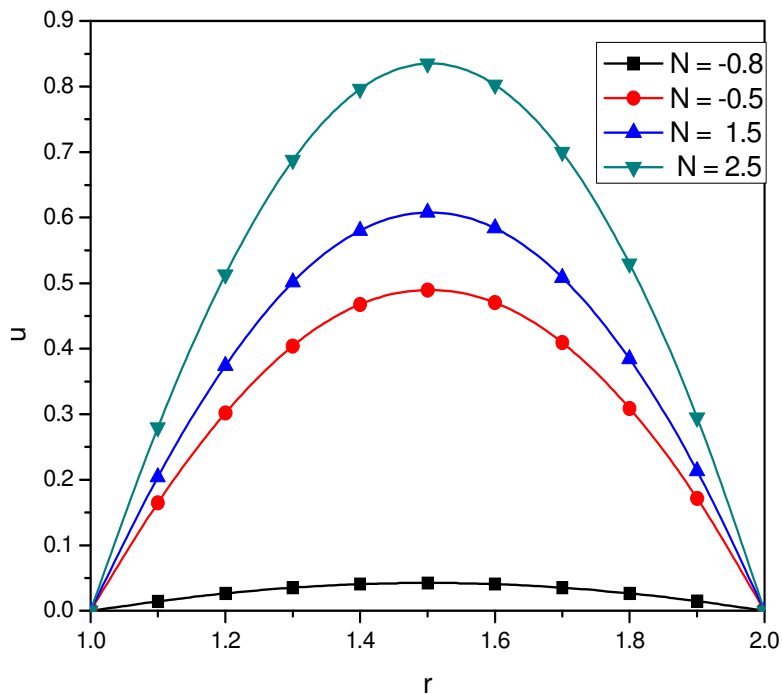


Figure 7. Variation of u with N $P = 0.71$, $Sr = 0.5$, $G = 2 \times 10^3$, $M = 2$, $D^{-1} = 2 \times 10^3$, $\alpha = 2$, $Du = 0.5$, $Ec = 0.01$, $Sc = 1.3$.

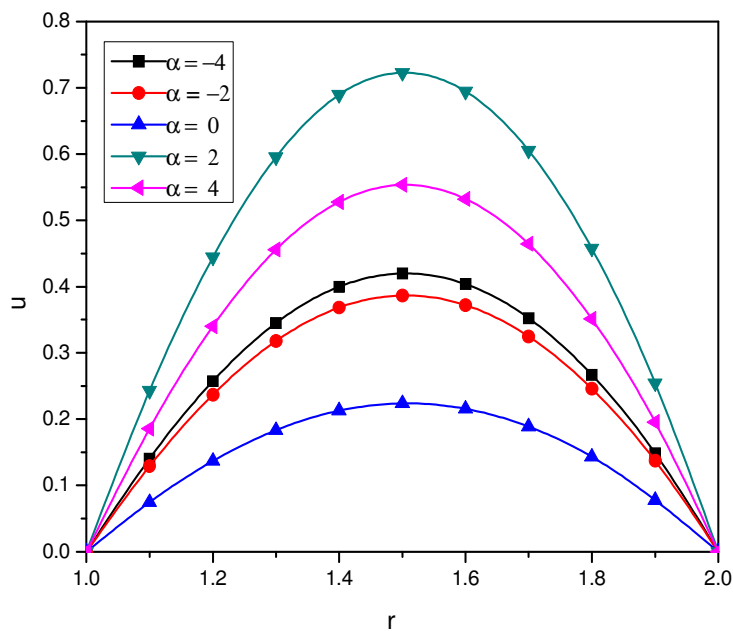


Figure 8. Variation of u with α $P = 0.71$, $Sr = 0.5$, $G = 2 \times 10^3$, $\alpha = 2$, $M = 2$, $N = 2$, $Du = 0.5$, $Ec = 0.01$, $Sc = 1.3$

in Du and $|u|$ enhances Du . The variation of u with N shows that when the molecular buoyancy force dominates over the thermal buoyancy force the actual axial velocity experiences a depreciation when the

buoyancy forces act in the same direction while for the forces acting in the opposite directions it experiences an enhancement in the flow region (Figure 7). The influence of heat source parameter α on u is shown in Figure 8. An

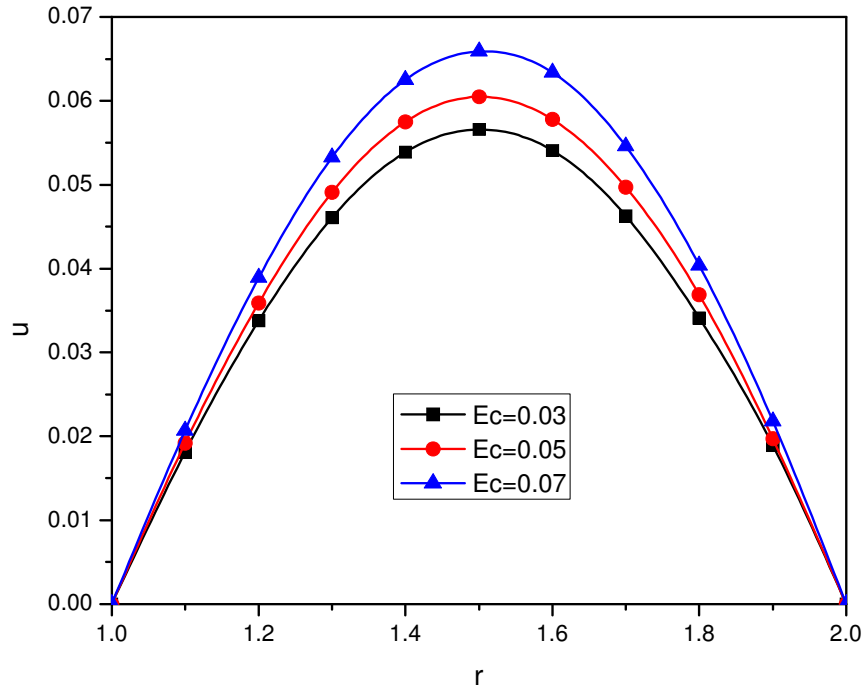


Figure 9. Variation of u with Ec $P = 0.71$, $Sr = 0.5$, $G = 2 \times 10^3$, $M = 2$, $N = 2$, $Du = 0.5$, $\alpha = 2$, $Ec = 0.01$, $Sc = 1.3$.

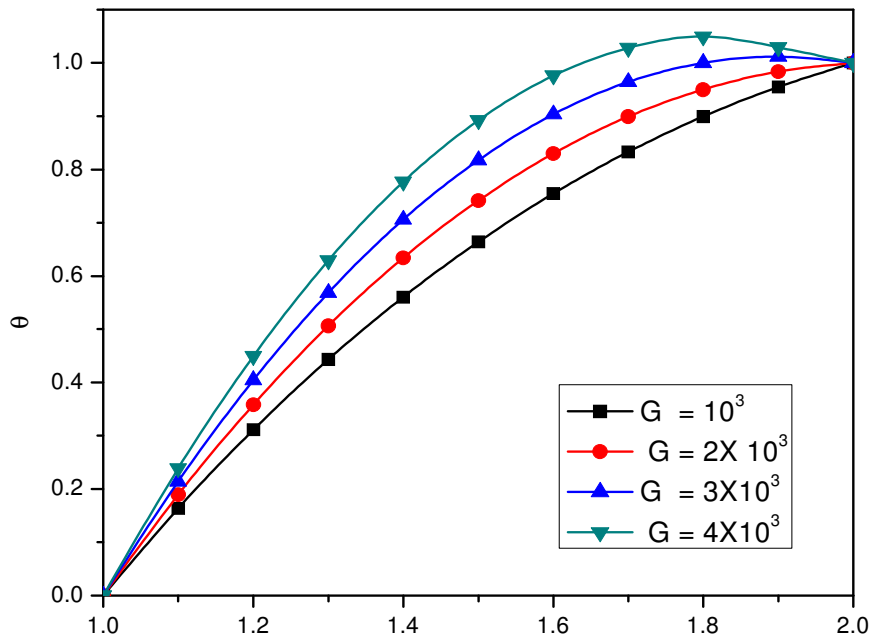


Figure 10. Variation of θ with G $P = 0.71$, $Sr = 0.5$, $D^{-1} = 2 \times 10^3$, $M = 2$, $\alpha = 2$, $N = 2$, $Du = 0.5$, $Ec = 0.01$, $Sc = 1.3$.

increase in $\alpha < 0$ enhances the actual axial velocity u that in the presence of the temperature, heat u is shown source depreciates the velocity in the flow region with maximum in the mid region. The influence of dissipative

effect on u is shown in Figure 9. We conclude that the axial velocity u experiences an enhancement with Ec . The non-dimension temperature (8) is shown in Figures 10- 18 for different values of the parameters. It is found

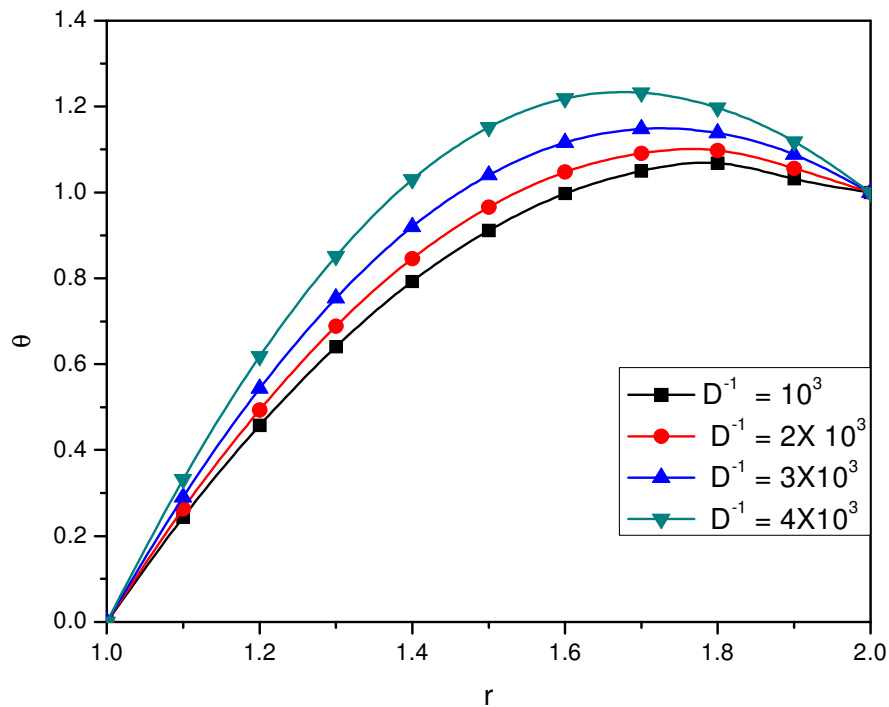


Figure 11. Variation of θ with $D^{-1}P = 0.71$, $Sr = 0.5$, $G = 2 \times 10^3$, $\alpha = 2$, $M = 2$, $N = 2$, $Du = 0.5$, $Ec = 0.01$, $Sc = 1.3$.

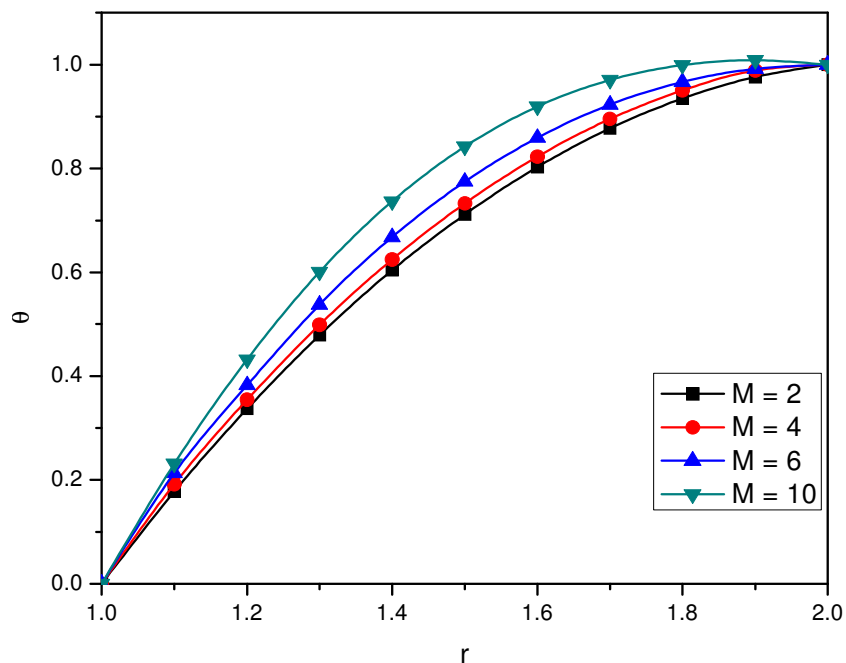


Figure 12. Variation of θ with $M P = 0.71$, $Sr = 0.5$, $G = 2 \times 10^3$, $D^{-1} = 2 \times 10^3$, $N = 2$, $\alpha = 2$, $Du = 0.5$, $Ec = 0.01$, $Sc = 1.3$.

that the non-dimensional temperature gradually increases from its prescribed value 0 on $r = 1$ to attain its prescribed value 1 at $r = 2$. An increase in G enhances the tem-

perature (Figure 10). The variation of θ with D^{-1} shows that the lesser the permeability of porous medium, the larger the temperature in the flow region (Figure 11).

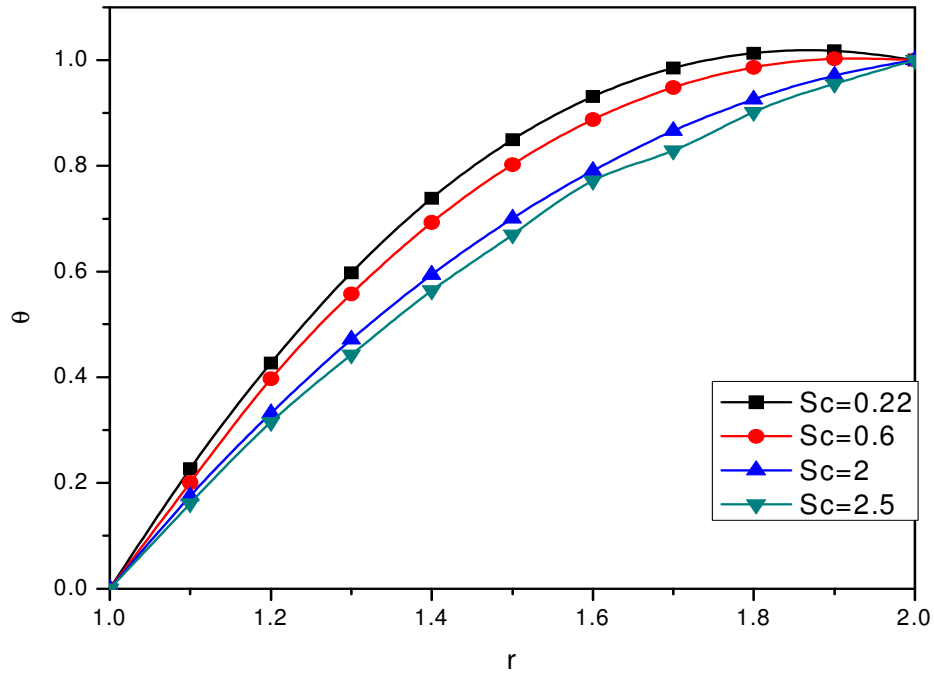


Figure 13. Variation of θ with Sc $P = 0.71$, $Sr = 0.5$, $G = 2 \times 10^3$, $M = 2$, $\alpha = 2$, $N = 2$, $Du = 0.5$, $Ec = 0.01$, $D^{-1} = 2 \times 10^3$.

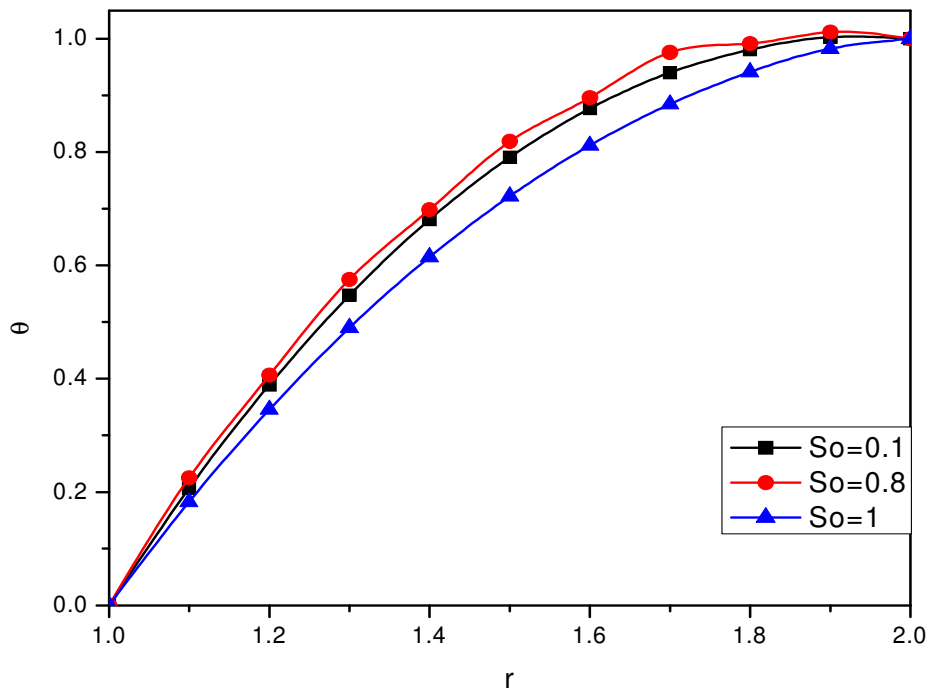


Figure 14. Variation of θ with So $P = 0.71$, $D^{-1} = 2 \times 10^3$, $G = 2 \times 10^3$, $M = 2$, $N = 2$, $\alpha = 2$, $Du = 0.5$, $Ec = 0.01$, $Sc = 1.3$.

From Figure 12 we find that lesser the Lorentz force larger the temperature. With respect to Sc we notice that lesser the molecular diffusivity smaller the temperature

in the flow region (Figure 13). An increase in Soret parameter Sr results in a depreciation in the actual temperature in the region (Figure 14). The variation of θ

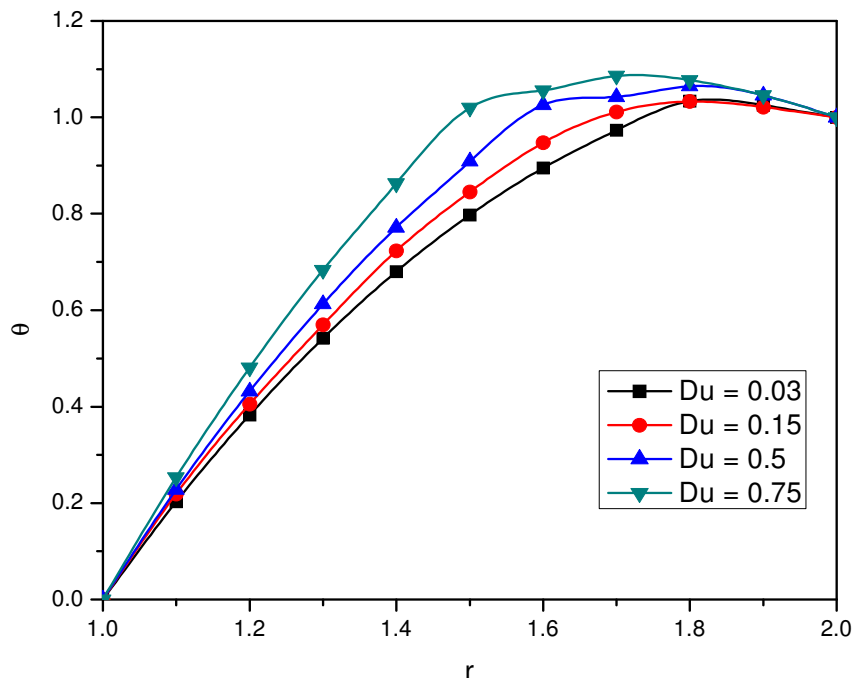


Figure 15. Variation of θ with Du $P = 0.71$, $Sr = 0.5$, $G = 2 \times 10^3$, $M = 2$, $N = 2$, $\alpha = 2$, $D^{-1} = 2 \times 10^3$, $Ec = 0.01$, $Sc = 1.3$.

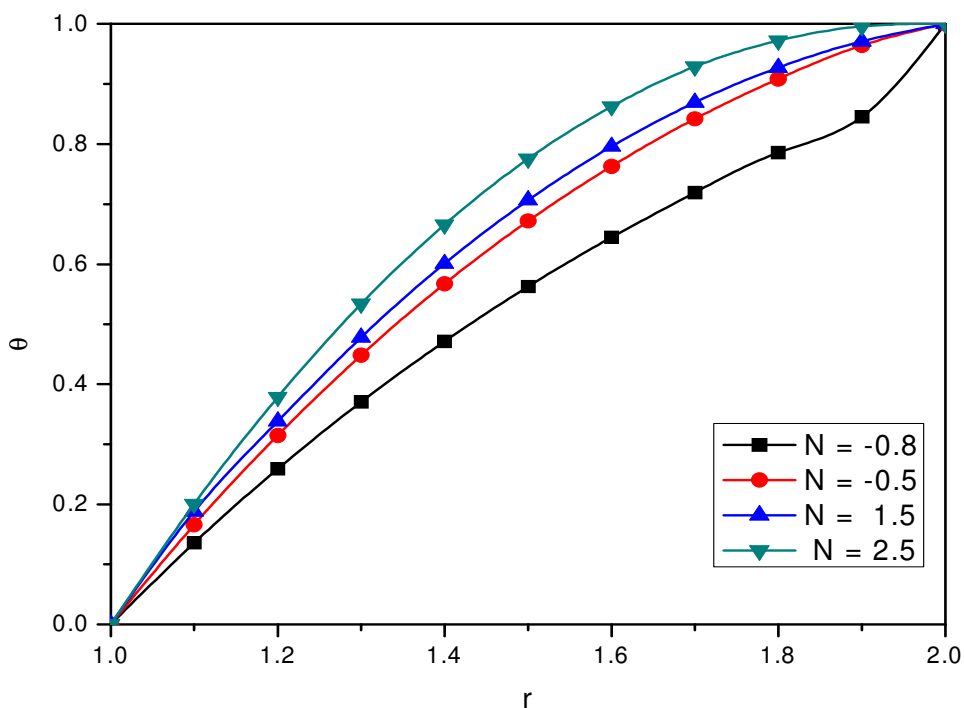


Figure 16. Variation of θ with N $P = 0.71$, $Sr = 0.5$, $G = 2 \times 10^3$, $M = 2$, $D^{-1} = 2 \times 10^3$, $\alpha = 2$, $Du = 0.5$, $Ec = 0.01$, $Sc = 1.3$.

with Dufour parameter Du shows that the actual temperature enhances gradually with increase in Du (Figure 15). When the molecular buoyancy force

dominates over the thermal buoyancy force the actual temperature decreases irrespective of the directions of the buoyancy forces (Figure 16). The influence of

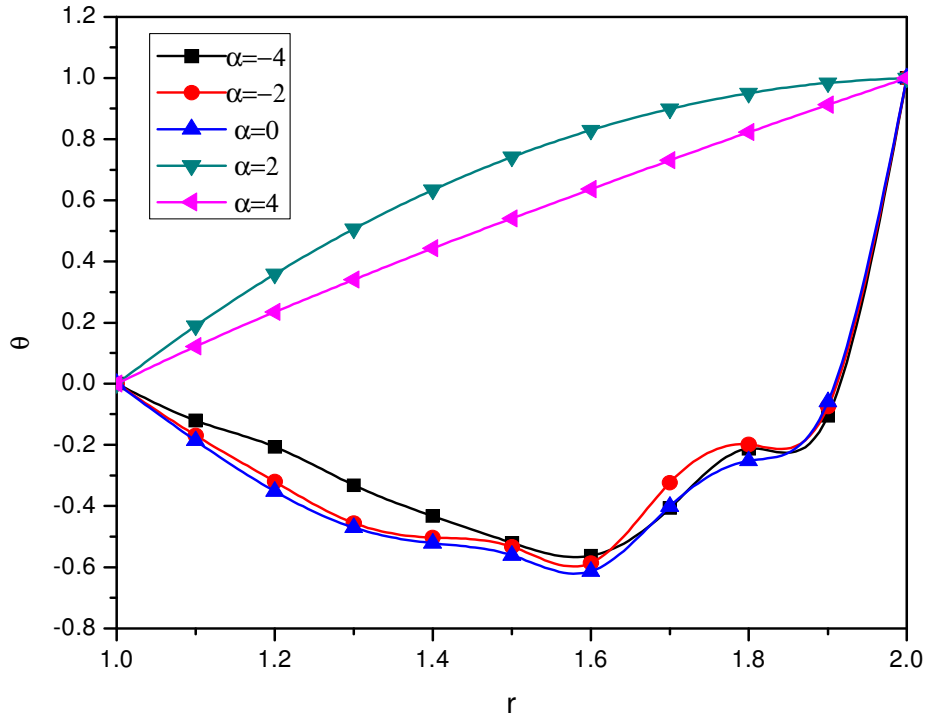


Figure 17. Variation of θ with α $P = 0.71$, $Sr = 0.5$, $G = 2 \times 10^3$, $\alpha = 2$, $M = 2$, $N = 2$, $Du = 0.5$, $Ec = 0.01$, $Sc = 1.3$.

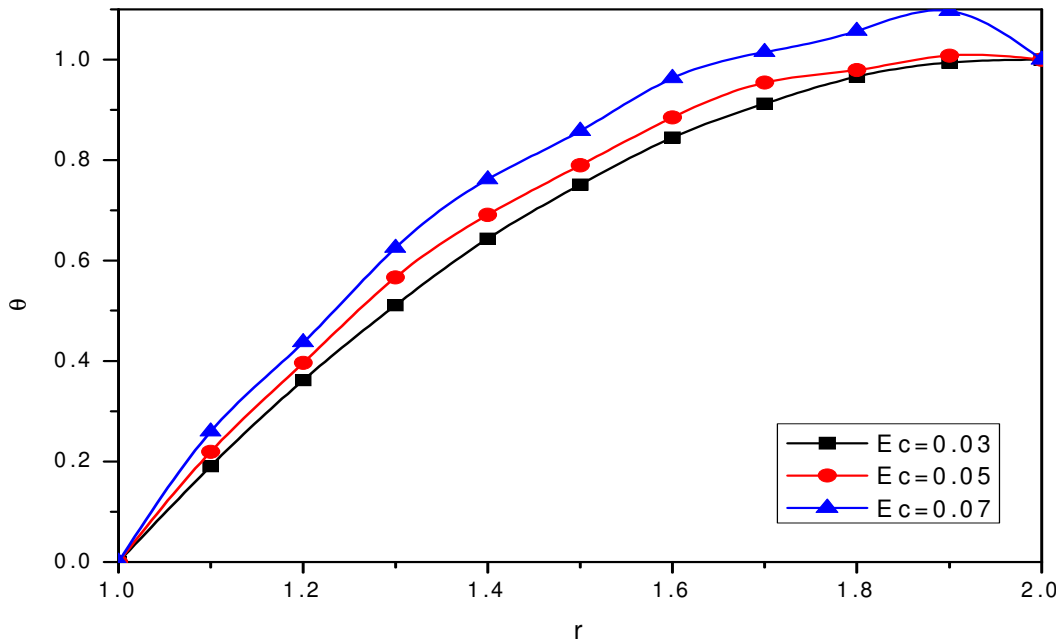


Figure 18. Variation of θ with Ec $P = 0.71$, $Sr = 0.5$, $G = 2 \times 10^3$, $M = 2$, $N = 2$, $Du = 0.5$, $\alpha = 2$, $Ec = 0.01$, $Sc = 1.3$.

temperature gradient heat source parameter α on θ is shown in Figure 17. It is found that the temperature is negative for $\alpha = 0$, $\alpha < 0$ and positive for $\alpha > 0$. The actual

temperature experiences depreciation with increase in the strength of the heat sources. The variation of θ with Eckert number Ec is shown in Figure 18. We found that

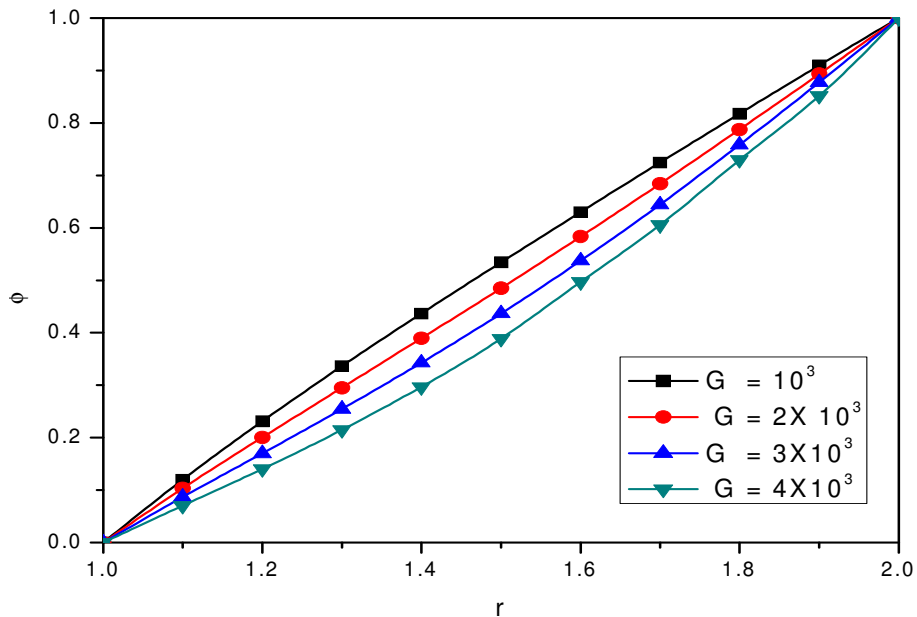


Figure 19. Variation of ϕ with $GP = 0.71$, $Sr = 0.5$, $D^{-1} = 2 \times 10^3$, $M = 2$, $\alpha = 2$, $N = 2$, $Du = 0.5$, $Ec = 0.01$, $Sc = 1.3$.

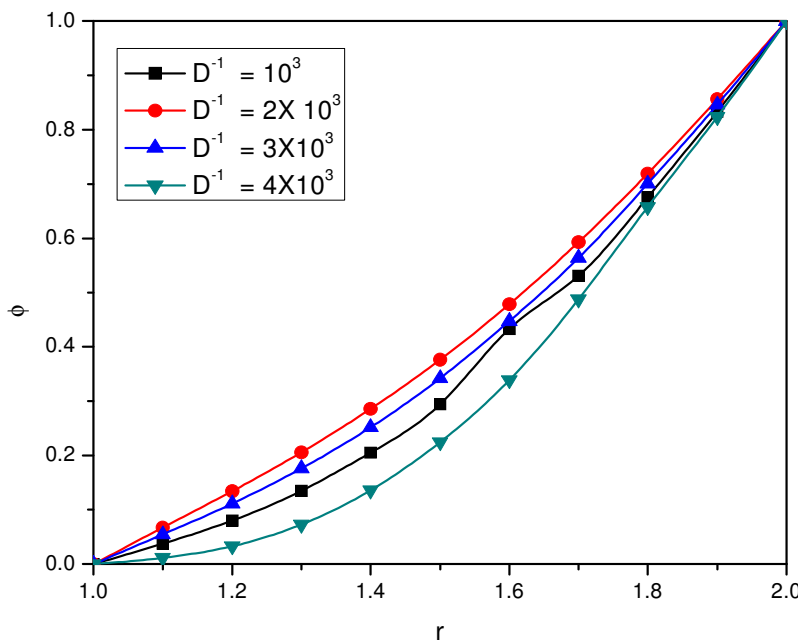


Figure 20. Variation of ϕ with $D^{-1} P = 0.71$, $Sr = 0.5$, $G = 2 \times 10^3$, $\alpha = 2$, $M = 2$, $N = 2$, $Du = 0.5$, $Ec = 0.01$, $Sc = 1.3$.

the actual temperature enhances increase in Ec .

The non-dimensional concentration (ϕ) is shown in Figures 19-27 for different values of the parameters G , D^{-1} , M , Sc , Sr , Du , N , α and Ec . It is found that the non-dimensional concentration gradually increases from its prescribed value 0 on $r = 1$ and attain its prescribed value 1 at $r = 2$. Figure 19 shows the variation of ϕ with G . It is

noticed that the concentration depreciates with increase in the Grashof number G . The variation of ϕ with D^{-1} shows that the lesser the permeability of porous medium, the higher the actual concentration in the flow region; and for further lowering of the permeability, the smaller the actual concentration in the flow region (Figure 20). From Figure 21 we found that the higher the Lorentz force, the

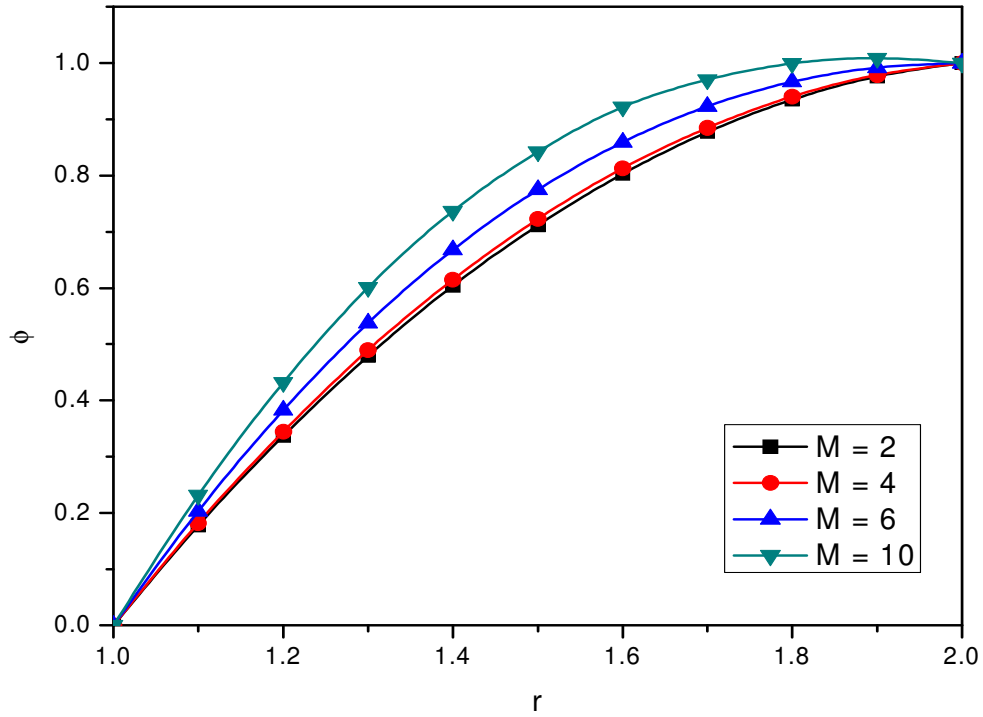


Figure 21. Variation of ϕ with $MP = 0.71$, $Sr = 0.5$, $G = 2 \times 10^3$, $D^{-1} = 2 \times 10^3$, $N = 2$, $\alpha = 2$, $Du = 0.5$, $Ec = 0.01$, $Sc = 1.3$.

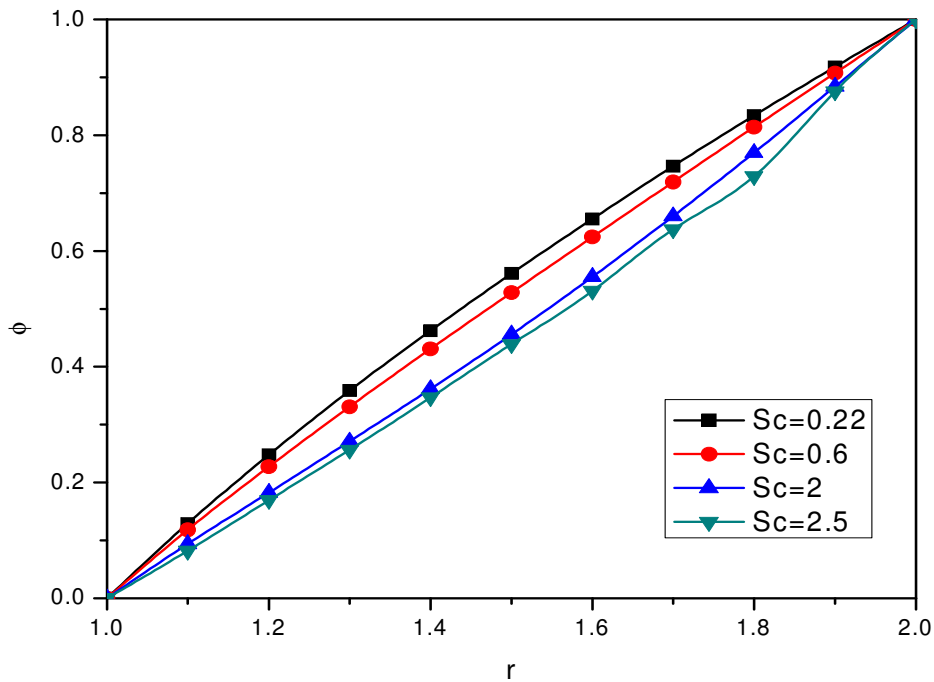


Figure 22. Variation of ϕ with $ScP = 0.71$, $Sr = 0.5$, $G = 2 \times 10^3$, $M = 2$, $\alpha = 2$, $N = 2$, $Du = 0.5$, $Ec = 0.01$, $D^{-1} = 2 \times 10^3$.

larger the concentration in the flow region. The lesser the molecular diffusivity is, the smaller the concentration

in the flow field (Figure 22). An increase in the Soret parameter Sr enhances the concentration everywhere in

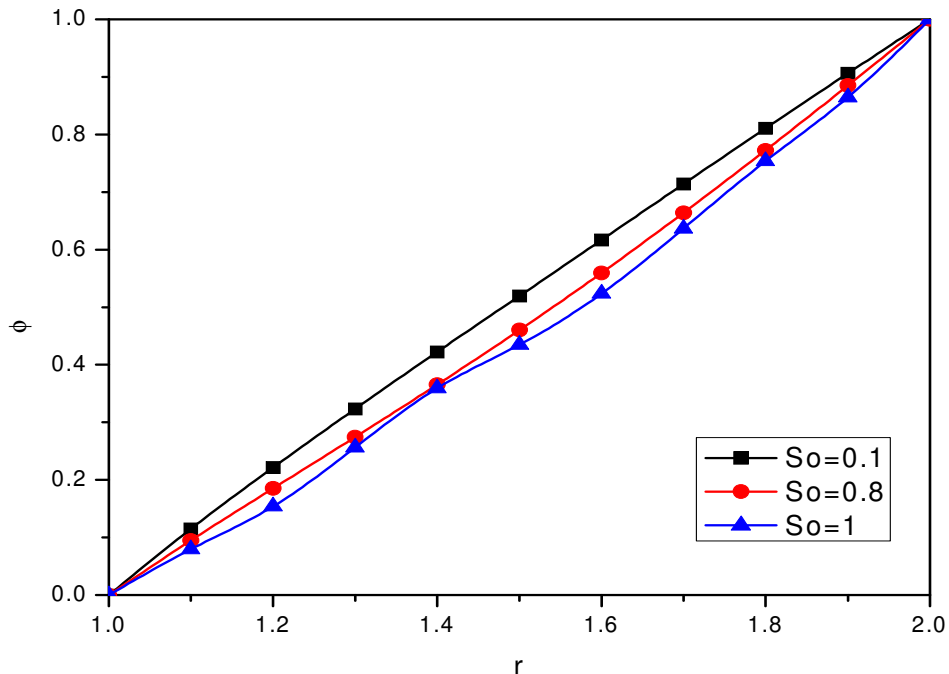


Figure 23. Variation of ϕ with So $P = 0.71$, $D^{-1} = 2 \times 10^3$, $G = 2 \times 10^3$, $M = 2$, $N = 2$, $\alpha = 2$, $Du = 0.5$, $Ec = 0.01$, $Sc = 1.3$.

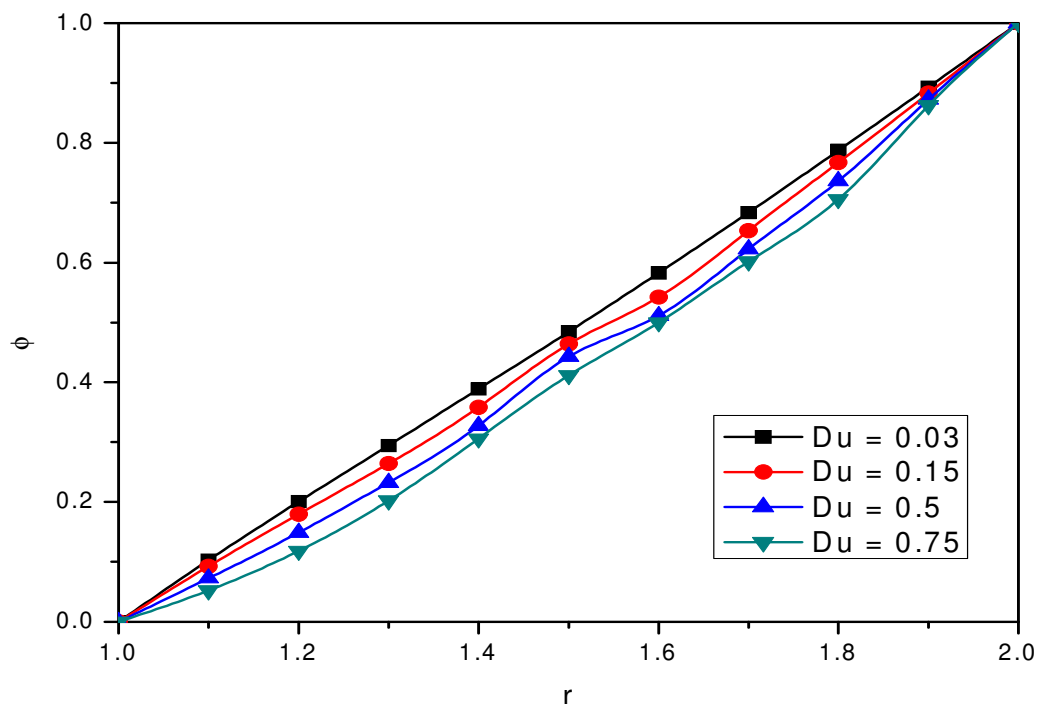


Figure 24. Variation of ϕ with Du $P = 0.71$, $Sr = 0.5$, $G = 2 \times 10^3$, $M = 2$, $N = 2$, $\alpha = 2$, $D^{-1} = 2 \times 10^3$, $Ec = 0.01$, $Sc = 1.3$.

the flow region (Figure 23). The variation of ϕ with Dufour parameter Du shows that the concentration experiences a marginal depreciation in the flow region (Figure 24).

The variation of ϕ with N shows that when the molecular buoyancy force dominates over the thermal buoyancy force the actual concentration experiences an

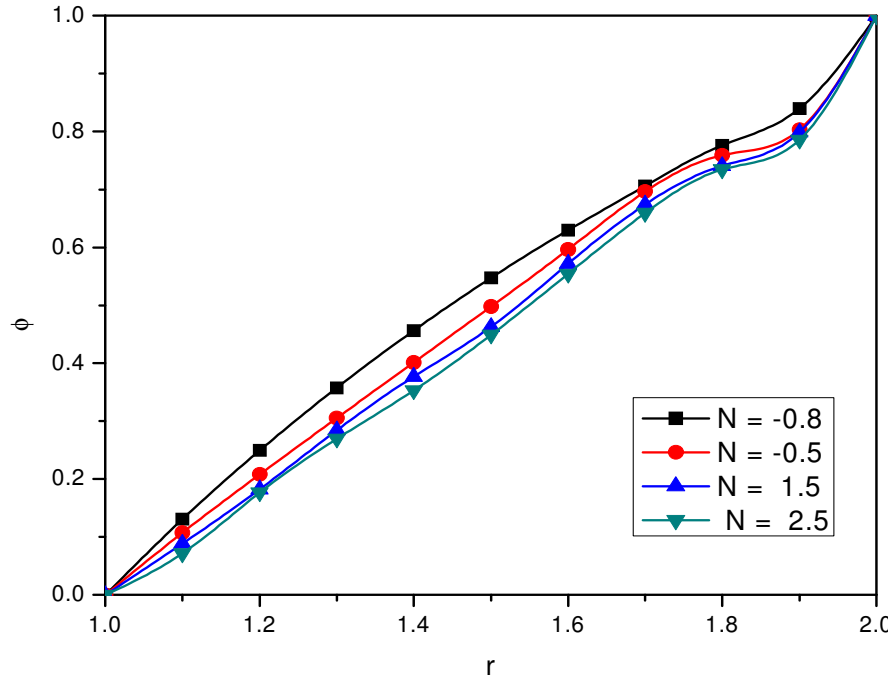


Figure 25. Variation of ϕ with $NP = 0.71$, $Sr = 0.5$, $G = 2 \times 10^3$, $M = 2$, $D^{-1} = 2 \times 10^3$, $\alpha = 2$, $Du = 0.5$, $Ec = 0.01$, $Sc = 1.3$.

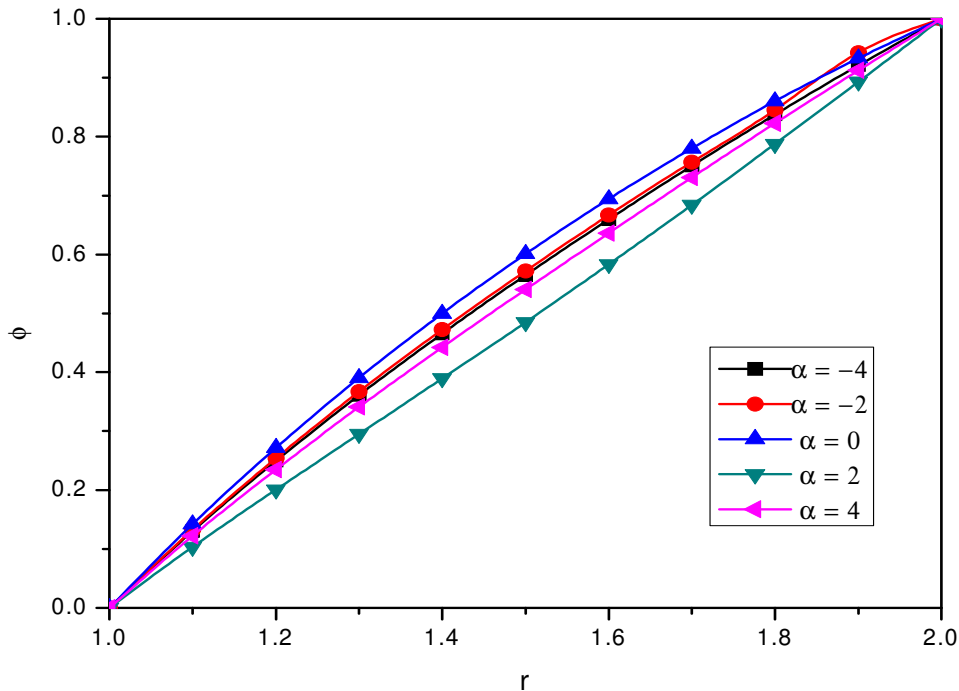


Figure 26. Variation of ϕ with $\alpha P = 0.71$, $Sr = 0.5$, $G = 2 \times 10^3$, $\alpha = 2$, $M = 2$, $N = 2$, $Du = 0.5$, $Ec = 0.01$, $Sc = 1.3$.

enhancement when the buoyancy forces act in the same direction while for the forces acting in the opposite directions it experiences depreciation in the flow region

(Figure 25). From Figure 26, we observe that ϕ experiences a marginal enhancement with $\alpha > 0$ and depreciation with $\alpha < 0$. The inclusion of the dissipation in

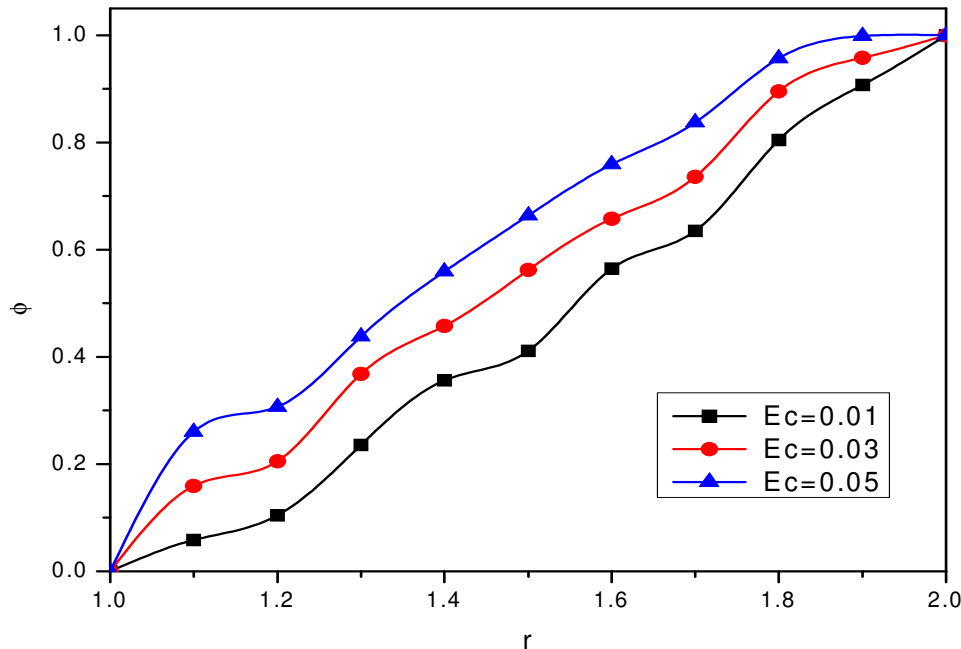


Figure 27. Variation of ϕ with Ec $P = 0.71$, $Sr = 0.5$, $G = 2 \times 10^3$, $M = 2$, $N = 2$, $Du = 0.5$, $\alpha = 2$, $Ec = 0.01$, $Sc = 1.3$.

the flow enhances the concentration in the flow region (Figure 27).

REFERENCES

- Anghel M, Takhar HS, Pop I (2000). Dofour, Soret effects on free convection boundary layer over a vertical surface embedded in a porous medium. *Studia universitates- Bolyai, Mathematica*, 45: 11-21.
- Barletta A, Lazzari S (2008). Mixed convection with heating effects in a vertical porous annulus with a radially varying magnetic field.
- Bejan A, Khair KR (1985). Heat and mass transfer by natural convection in a porous medium., *Int. J. Heat and mass transfer*, 5(28): 908-818.
- Brinkman HC (1948). A Calculation of the viscous force exerted by a flowing fluid on a dense swarm of particles. *Appl. Science Res., Ala*, p. 81.
- Chandra SS (1961). *Hydrodynamic and Hydro magnetic stability*, Clarendon press, oxford.
- Emmanuel O, Jonathan S, Robert H (2008). "Thermal-diffusion and diffusion thermo effects on combined heat and mass transfer of a steady MHD convective and slip flow due to a rotating disk with viscous dissipation and ohmic heating: *Int. Commun. Heat Mass Transfer*, 35: 908-915.
- Gokhale MY, Behnaz-Farnam (2007). "Transient free convection flow on an isothermal plate with temperature dependent heat sources", *International review of Pure and Applied Mathematics*, 3(1): 129-136.
- Jang JY, Chang WJ (1987). The flow and vortex instability of horizontal natural convection in a porous medium resulting from combined heat and mass buoyancy effects. *Int. Heat Mass Transfer*, 5(31): 769-777.
- Muthukumara, Swamy, Maheswari J, Pandurangan J (2007). "Study of MHD and Radiation effects on moving vertical plate with variable temperature and mass diffusion", *Int. Rev. Pure Appl. Math.*, 3(1): 95-103.
- Nanda RS, Mohan M (1978). *Proc. Ind Acad. Sci.*, 876 A(5): 147.
- Prasad V (1984). Natural convection in a vertical porous annulus, *Int. J. Heat and Mass Transfer*, 27: 207-219.
- Prasad V, Kulacki FA (1985). Natural convection in porous media bounded by short concentric vertical cylinders, *ASME J. Heat Transfer*, 107: 147-154.
- Prasad V, Kulacki FA, Keyhani M (1985). Natural convection in porous media, *J. fluid mech.*, 150: 89-119.
- Saffman PG (1971). On the boundary conditions at the free surface of a porous medium. *Stud. Appl. Maths*, 2: 93.
- Sallam N (2009). *Thermal-Diffusion and Diffusion-Thermo Effects on Mixed Convection Heat and Mass transfer in a Porous Medium. J. Porous Media*.
- Sivaiah (2004). *Thermo-diffusion effect on convective heat and mass transfer flow through a porous medium in ducts. Ph.D thesis, S.K. University, Anantapur.*
- Sreevani M (2003). *Mixed convection heat and mass transfer through a porous medium in channels with dissipative effects, Ph.D thesis S.K. University, Anantpur, India.*
- Vasseur P, Nguyen TH, Robillard, Thi VKT (1984). *Int. Heat Mass Transfer*, 27: 337.
- Verschoor (1992). *Int. Heat Mass Transfer*, p. 31.